

Prediction of impact sensitivity of nitro energetic compounds by neural network based on electrotopological-state indices

Rui Wang, Juncheng Jiang*, Yong Pan, Hongyin Cao, Yi Cui

Jiangsu Key Laboratory of Urban and Industrial Safety, Institute of Safety Engineering, Nanjing University of Technology, Nanjing 210009, China

ARTICLE INFO

Article history:

Received 18 July 2008

Received in revised form 4 November 2008

Accepted 4 November 2008

Available online 13 November 2008

Keywords:

Quantitative structure–property relationship

Electrotopological-state indices

Artificial neural network

Impact sensitivity

Nitro energetic compounds

ABSTRACT

A quantitative structure–property relationship (QSPR) model was constructed to predict the impact sensitivity of 156 nitro energetic compounds by means of artificial neural network (ANN). Electrotopological-state indices (ETSI) were used as molecular structure descriptors which combined together both electronic and topological characteristics of the analyzed molecules. The typical back-propagation neural network (BPNN) was employed for fitting the possible non-linear relationship existed between the ETSI and impact sensitivity. The dataset of 156 nitro compounds was randomly divided into a training set (64), a validation set (63) and a prediction set (29). The optimal condition of the neural network was obtained by adjusting various parameters by trial-and-error. Simulated with the final optimum BP neural network [16–12–1], the results show that most of the predicted impact sensitivity values are in good agreement with the experimental data, which are superior to those obtained by multiple linear regression (MLR) and partial least squares (PLS). The model proposed can be used not only to reveal the quantitative relation between impact sensitivity and molecular structures of nitro energetic compounds, but also to predict the impact sensitivity of nitro compounds for engineering.

© 2008 Elsevier B.V. All rights reserved.

1. Introduction

Prediction of sensitivity is of great importance in deriving novel energetic molecules because safe handling is one of the most important issues to the scientists and engineers who handle energetic molecules [1]. Some stimulation, which includes impact, shock, heat, electrostatic discharge and friction, can cause detonation. Among various aspects of sensitivity, impact sensitivity is one of the most basic and important properties of energetic molecules. Experimentally, impact sensitivity is measured by drop-weight impact test, where a 2.5 kg weight is dropped from a predetermined height onto the striker plate and evidence of reaction or no reaction is recorded. A sequence of test is carried out till the impact sensitivity or the sensitivity index, H_{50} is obtained. The H_{50} is the height that a given weight dropped onto the sample produce an explosion of 50% the test trails.

The study on the correlation between impact sensitivity and the structure of energetic molecules has been an ongoing research field in explosive theory [2]. Kamlet and Adolph [3] found reasonable linear correlations between oxygen balance OB_{100} and

$\log H_{50}$ for families of high energy molecules with similar decomposition mechanisms. Politzer and coauthors [4–9] have identified some features of electrostatic potentials using quantum mechanical calculations for $C_aH_bN_cO_d$ explosives that appeared to be related to their sensitivity impact. Rice and Hare [10] used approximations to the electrostatic potential at midpoints, statistical parameters of these surface potentials and the property–structure relation method “generalized interaction property function” or computed heats of detonation to predict impact sensitivity of $C_aH_bN_cO_d$ explosives and established five models. Xiao and coworkers [11–16] used quantum chemistry calculation to propose the thermodynamic criteria of “the smallest bond order”, “the principle of the easiest transition”, and the kinetic criterion of “the reaction activation energy of pyrolysis initiation” to judge the impact sensitivity. Zhang et al. [17–19] on the basis of DFT have found some relationships between impact sensitivity and nitro group charges. Keshavarz [20] found some structural parameters to predict the impact sensitivity of nitrate, nitroaliphatic and the derivatives.

Artificial neural networks (ANN) architectures have been recently used as prediction methodology for impact sensitivity. Nefati et al. [21] first introduced the ANN to the prediction of energetic molecules. Cho et al. [22] optimized the ANN architecture based on the Nefati’s work. Keshavarz and Jaafari [23] built an ANN model by choosing new descriptors as input parameters, and the model showed a better prediction as compared to the quantum mechanical models of Rice and Hare [10].

* Corresponding author at: Mail Box 186, No. 5 Ximofan Road, Nanjing University of Technology, Nanjing 210009, China. Tel.: +86 25 83587305; fax: +86 25 83587411.

E-mail addresses: po.sai.don@hotmail.com (R. Wang), ypnjut@126.com, rcjiang@njut.edu.cn (J. Jiang), yongpannjut@163.com (Y. Pan), dajiao517@sohu.com (H. Cao), flyan0208@163.com (Y. Cui).

In this study, the well-accepted quantitative structure–property relationship (QSPR) method is employed to investigate the quantitative correlation between the impact sensitivity and molecule structures of nitro energetic compounds. QSPR is a mathematical method that relates the properties of interest to the molecular structures of compounds which are represented by a variety of molecular descriptors. Molecular descriptors are various molecular-based theoretical parameters which can be calculated using known mathematical algorithms solely from molecular structures. In this study, the widely used electrotopological-state indices (ETSI) were employed as descriptors to encode the structure characters of the studied compounds. The atom-type E-state indices were introduced by Hall and Kier [24] for the first time as an atomic level molecule descriptors. Indices of this kind combine the electronic and topological characters together. Furthermore, they take into account the surrounding chemical environment of atoms in the molecule. Thus the ETSI have been proved effective in predicting many physical and chemical properties of pure compounds, such as the critical temperature [25], boiling point [24,25], aqueous solubility [26,27], partition coefficient [28], log *P* [29], toxicity [30], auto ignition point [31], and so on. However, to our best knowledge there has no attempts been made to predict the sensitivity of energetic compounds by employing the ETSI.

The main goal of this work is to investigate the feasibility and efficiency of ETSI in predicting the impact sensitivity of nitro energetic compounds. By employing two linear modeling methods of multiple linear regressions (MLR) and partial least squares (PLS), as well as a non-linear artificial neural network (ANN) method, we wish that the present study would be a new attempt for predicting the impact sensitivity from molecular structures, and would improve the prediction results.

2. Materials and methods

2.1. Dataset

The whole dataset is extracted from the literatures, which consists of 156 compounds containing C, H, O and N. 138 of the impact sensitivity were collected from the Explosive Research Laboratory (U.S.A.) [32] providing the largest number of impact sensitivity measurements currently available; 16 of them were taken from literature [4] and the rest 2 from [3]. The impact sensitivity is measured by the logarithmic 50% impact height, lg *H*₅₀. Compounds with lg *H*₅₀ > 2.5 (*H*₅₀ > 320 cm) from literature [32] were discarded since their sensitivity did not have specified values. The compounds finally selected in the dataset belong to several families: 49 nitroaromatics, 55 nitramine, 40 nitroaliphatic compounds containing other functional groups, 7 nitrate esters, and 5 nitroaliphatic compounds. Besides, it must be stated that the polynitroheterocycles are not taken into account in this study due to their special structures and different detonation mechanism. However, the studied dataset employed in this work are also named as “nitro energetic compounds” for the purpose of convenience and avoiding prolixity.

The dataset was randomly divided into a training set with 127 compounds and a prediction set with 29 compounds. The training set was used for model development, and the prediction set for model validation. In addition, for comparison purpose, both the training set and prediction set for all the three modeling methods consisted of the same compounds.

2.2. Molecular descriptors

What is known as a critical aspect of QSPR research is the selection of suitable molecule descriptors. An efficient descriptor should reflect as much structural information as possible and the more

Table 1

The symbols of 16 kinds of ETSI descriptors.

Number	Descriptor type	ETSI symbol	Descriptors
1	aCHa	SaaCH	<i>X</i> ₁
2	saCa	SsaaC	<i>X</i> ₂
3	–N<<	SddsN	<i>X</i> ₃
4	=O	SdO	<i>X</i> ₄
5	>C<	SssssC	<i>X</i> ₅
6	–N<	SsssN	<i>X</i> ₆
7	–NH–	SssNH	<i>X</i> ₇
8	–CH<	SsssCH	<i>X</i> ₈
9	–CH ₂ –	SssCH ₂	<i>X</i> ₉
10	–CH ₃	SsCH ₃	<i>X</i> ₁₀
11	–Cl	SsCl	<i>X</i> ₁₁
12	–OH	SsOH	<i>X</i> ₁₂
13	–O–	SssO	<i>X</i> ₁₃
14	–NH ₂	SsNH ₂	<i>X</i> ₁₄
15	>C=	SdssC	<i>X</i> ₁₅
16	–NO ₂	S(–NO ₂)	<i>X</i> ₁₆

precise the better. In this paper we employed the widely used atom-type ETSI [24], which combine together the electronic and topological characters of a molecule and take the binding environment into account. For each atom type in a molecule, the ETSI were summed up and lent itself for use in a group additive type scheme in which an index appeared for each atom type in the molecule (together with its electrotopological-state contribution). Base on the methodology of constructing the atom-type ETSI, we also introduced the group-type ETSI with the consideration that nitro group had significant influence of impact sensitivity. The group-type ETSI were calculated by summing the electrotopological-state values of all the atoms constructed the analyzed functional groups. The detailed description on the procedure of calculation of the ETSI can refer to the original work of Hall and Kier [24]. For the 156 nitro energetic molecules studied in this paper, a total of 16 kinds of ETSI descriptors were selected, which include 15 atom-type ETSI descriptors and one group-type ETSI descriptor. The detailed ETSI symbols were listed in Table 1.

2.3. Modeling methods

In this work, three methods were employed to build the QSPR models between the ETSI descriptors and the impact sensitivity of nitro energetic compounds. Two of the methods were linear techniques of multiple linear regressions (MLR) and partial least squares (PLS). The other one was artificial neural networks (ANN) which had extensive applicability in solving non-linear systems.

The MLR analysis was performed by the SPSS software (Version 11.0; SPSS Inc.; Chicago, IL), and the PLS calculation was completed via the MATLAB program written in M-files.

The ANN model was built by the STATISTICA Neural Networks (SNN) software. A three-layer feed-forward neural network utilizing the back-propagation algorithm was employed. The typical back-propagation network consists of an input layer, an output layer and at least one hidden layer. Each layer contains neurons and each neuron is a simple micro-processing unit which receives and combines signals from many neurons. The illustration of the architectures of the ANN used in this study can be seen in Fig. 1. The number of neurons presented in the input and output layer depends on the number of variables (in this work ETSI and the impact sensitivity, respectively). Besides, the number of neurons used for the hidden layer is optimized by trial-and-error training assays.

Each neuron has weighted inputs, summation function, transfer function and output. The behavior of a back-propagation network is mainly determined by the transfer functions of its neurons. At first, summation function is computed from the weighted sum of all input neurons entering each hidden neuron and the weighted

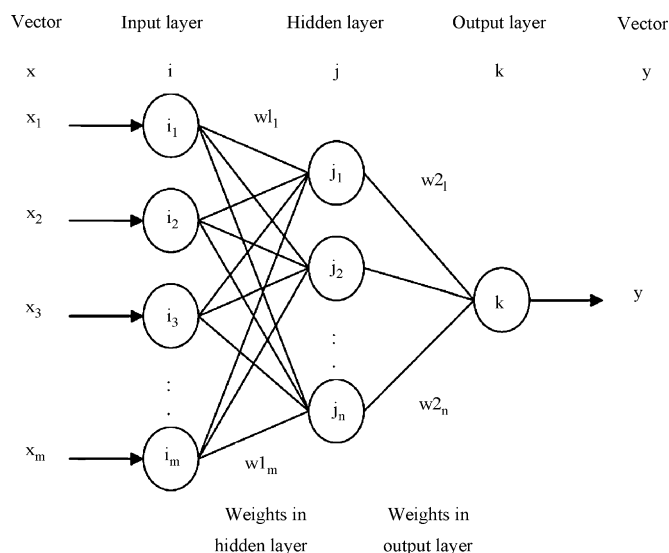


Fig. 1. The neural network architecture used in this work.

sum of the inputs constitutes the activation of the neuron. Then the activation signal is passed on to the transfer function for further processing. The role of the transfer function is to translate the summed information into outputs. In this work, a logistic $f(x) = 1/[1 + \exp(-x)]$ transfer function was applied both for hidden and output neurons.

For a given input and a desired output, the back-propagation neural network system can be trained by the following steps [33]:

- (1) The input vector is presented to the input layer of the network, and then propagates through the hidden layer to the output layer, where all of the summed inputs and output states for each processing element in the network are set and an output value is produced.

$$net_j^h = \sum_i \omega_{ij} O_i \quad (1)$$

$$O_j^h = f(net_j^h) = \frac{1}{[1 + \exp(-net_j^h)]} \quad (2)$$

$$net_k^o = \sum_j \omega_{jk} O_j^h \quad (3)$$

$$O_k^o = f(net_k^o) = \frac{1}{[1 + \exp(-net_k^o)]} \quad (4)$$

where, f is the sigmoid transfer function, and w_{ij}/w_{jk} are the connection weights between hidden units and input/output units.

- (2) The actual output value O_k^o is compared with the desired output value T_k , and the error E_p and the global error E are determined, respectively.

$$E_p = \frac{1}{2} \sum_k (T_{pk} - O_{pk}^o)^2 \quad (5)$$

$$E = \frac{1}{2p} \sum_p \sum_k (T_{pk} - O_{pk}^o)^2 \quad (6)$$

- (3) The weights are modified to reduce the error associated with the overall error function. In this work, gradient descent method is carried out for the reduction of E . The gradient descent method is an iterative least squares procedure which tries to adjust the connection weight for reducing the error most rapidly, by mov-

ing the state of the system downward towards the direction of maximum gradient.

$$\omega_{jk}(n+1) = \omega_{jk}(n) + \eta \delta_{pk} O_{pj} \quad (7)$$

$$\omega_{ij}(n+1) = \omega_{ij}(n) + \eta \delta_{pj} O_{pj} \quad (8)$$

$$\delta_{pk} = \frac{\partial E_p}{\partial net_k^o} = O_{pk}^o (1 - O_{pk}^o) (T_{pk} - O_{pk}^o) \quad (9)$$

$$\delta_{pj} = \frac{\partial E_p}{\partial net_j^h} = O_{pj}^h (1 - O_{pj}^h) \sum_k \delta_{pk} \omega_{jk} \quad (10)$$

- (4) For each hidden layer, the training process starts at the layer below the output layer, and ends with the layer above the input layer. And for each processing element in the hidden layer, the global error E is calculated and propagated back through the networks. Furthermore, the delta weights are calculated again.
- (5) Finally, in order to reduce the error, all of the weights in the networks are updated by adding the delta weights to the corresponding previous weights. And the training process of the ANN will be completed when the global error E is minimized.

Before the beginning of the training process, the optimal condition of the neural network was obtained by adjusting various parameters by trial-and-error. These parameters include: the learning rate, the momentum factor, the number of neurons in the hidden layer, and the training endpoint. The learning rate determines the speed at which the weights change. A large learning rate may cause instability of the prediction system, while a small one may lead to low convergence level. The momentum factor prevents sudden changes in attaining the results. These two parameters are usually set empirically, and in this study they were pre-optimized and both assigned as 0.01.

The optimal number of neurons in the hidden layer was determined by varying the number of hidden neurons and observing the root mean square error (RMS), which was used as a measure of the prediction error of the trained model and was calculated with the following equation:

$$RMS = \sqrt{\frac{\sum_{i=1}^n (p_i - a_i)^2}{n}} \quad (11)$$

where, n is the number of compounds in the dataset, and p_i is the predicted output, a_i is the actual output, respectively. Calculations of RMS were performed with leave-one-out cross-validation and the average RMS of 10 runs was adopted. Leave-one-out cross-validation referred to removing one sample in the dataset using for the test set while the rest using as training set. Such process was repeated until all samples of the dataset were used as the test sample. Finally, the number of neurons that gave the lowest RMS was selected, and 16–12–1 was chosen as the best network architecture in the presented work.

The early stopping technique was employed in the present study for avoidance of overfitting. For the determination of optimal training endpoint, a validation set contained 63 compounds was used to monitor the training process as measured by RMS. Thus, the training endpoint giving the lowest RMS for the predictions of the validation set was used.

2.4. Model validation

For the QSPR models, the quality was always judged by the statistical characters, for instance, the squared R (R^2) and the root mean square error (RMS). These parameters mainly reflect the goodness of fit of the models. However, recent studies [34,35] have indicated that good fitness could not automatically stand for good robustness and internal predictive ability, and thus internal validation

are considered to be necessary for model validation. In the present study, we took the leave-one-out (LOO) cross-validation (CV) for the internal validation to evaluate the internal predictive ability of developed models, and its result was defined as Q_{LOO}^2 , which could be calculated with the following equation [34]:

$$Q_{LOO}^2 = 1 - \frac{\sum_{i=1}^{\text{training}} (y_i - y'_i)^2}{\sum_{i=1}^{\text{training}} (y_i - \bar{y})^2} \quad (12)$$

where y_i , y'_i , and \bar{y} were respectively the experimental, predicted, and mean $\lg H_{50}$ values of the samples for the training set.

Moreover, as we known, the external validation is a significant and necessary validation method used to determine both the generalizability and the true predictive ability of the QSPR models for new chemicals, by splitting the available dataset into a training set and an external prediction set. As mentioned above, the whole dataset in this work has been randomly divided into a training set with 127 compounds for model development, and a prediction set with 29 compounds for model external validation. The external predictive ability of developed models on the external prediction set was evaluated by Q_{ext}^2 , which could be calculated with the following equation [34]:

$$Q_{\text{ext}}^2 = 1 - \frac{\sum_{i=1}^{\text{prediction}} (y_i - y'_i)^2}{\sum_{i=1}^{\text{prediction}} (y_i - \bar{y}_{tr})^2} \quad (13)$$

where y_i and y'_i were the experimental and predicted H_{50} values of the samples for the prediction set, and \bar{y}_{tr} was the mean experimental H_{50} values of the samples for the training set.

2.5. Hardware

All the calculations involved in this study are performed on a 2.4 GHz Intel Pentium IV with 2 GB RAM under windows XP.

3. Results and discussion

The linear techniques of MLR and PLS were carried out to develop QSPR models on the training set after the data standardization, and the resulted regression equations were listed as follows:

$$\begin{aligned} \lg H_{50} = & 1.4315 + 0.2095X_1 - 0.0563X_2 + 0.1601X_3 + 0.0146X_4 \\ & - 0.0656X_5 - 0.0352X_6 + 0.0515X_7 - 0.0193X_8 - 0.0707X_9 \\ & - 0.2347X_{10} - 0.0052X_{11} + 0.0079X_{12} + 0.0054X_{13} \\ & + 0.0695X_{14} + 0.0253X_{15} - 0.0107X_{16} \end{aligned} \quad (14)$$

$$R^2 = 0.7705, \text{ RMS} = 0.212, \text{ } n = 127 \text{ (MLR)}$$

$$\begin{aligned} \lg H_{50} = & 1.3729 + 0.2078X_1 - 0.0495X_2 + 0.1623X_3 + 0.0068X_4 \\ & - 0.0680X_5 - 0.0335X_6 + 0.0573X_7 - 0.0109X_8 - 0.0596X_9 \\ & - 0.2348X_{10} - 0.0055X_{11} + 0.0103X_{12} + 0.0083X_{13} \\ & + 0.0711X_{14} + 0.0123X_{15} - 0.0012X_{16} \end{aligned} \quad (15)$$

$$R^2 = 0.7659, \text{ RMS} = 0.214, \text{ } n = 127 \text{ (PLS)}$$

In the equations, n is the number of compounds used for model building. The two equations are then used to predict the impact sensitivity values of the compounds in the prediction set for external validation. Finally, the predicted impact sensitivity values for all 156 compounds are obtained and presented in Table 2. The main performance parameters of both models are shown in Table 3. A plot of the predicted impact sensitivity values versus the experimental ones for both models are shown in Figs. 2 and 3.

As can be seen from Table 3, the performance of both linear models developed over the whole dataset was not good as expected. So, in order to obtain more effective models, the dataset was divided into three main classes according to their chemical families for developing new models. Because the nitrate esters are only 7 cases with 9 descriptors, which cannot be used for a regression and curve fitting, so we combine them with the nitroaliphatic compounds. As a result, the resulted three new datasets are nitroaromatic compounds, nitramine compounds and nitroaliphatic compounds (together with compounds containing other functional groups). In addition, the three new datasets were also divided into a training set and a prediction set according to the original divisions. Finally, the resulted equations for the three new datasets were obtained and listed as follows:

$$\begin{aligned} \lg H_{50} = & 1.7618 + 0.1559X_1 - 0.0376X_2 + 0.1269X_3 - 0.0500X_4 \\ & - 0.0931X_5 - 0.0771X_7 + 0.1288X_8 + 0.1368X_9 + 0.1077X_{10} \\ & - 0.040X_{11} - 0.0026X_{12} + 0.0462X_{13} + 0.0479X_{14} \\ & - 0.3240X_{15} + 0.0565X_{16} \end{aligned} \quad (16)$$

$$R^2 = 0.8397, \text{ RMS} = 0.1477, \text{ } n = 39 \text{ (MLR)}$$

$$\begin{aligned} \lg H_{50} = & 1.7618 + 0.1559X_1 - 0.0376X_2 + 0.1269X_3 - 0.0500X_4 \\ & - 0.0931X_5 - 0.0771X_7 + 0.1288X_8 + 0.1368X_9 + 0.1077X_{10} \\ & - 0.040X_{11} - 0.0026X_{12} + 0.0462X_{13} + 0.0479X_{14} \\ & - 0.3240X_{15} + 0.0565X_{16} \end{aligned} \quad (17)$$

$$R^2 = 0.8346, \text{ RMS} = 0.150, \text{ } n = 39 \text{ (PLS)}$$

$$\begin{aligned} \lg H_{50} = & 0.9522 + 0.1093X_3 - 0.0256X_4 + 0.0216X_5 + 0.0294X_6 \\ & + 0.1048X_7 - 0.0628X_9 + 0.4057X_{10} + 0.0188X_{13} \\ & + 0.1055X_{15} - 0.0190X_{16} \end{aligned} \quad (18)$$

$$R^2 = 0.8522, \text{ RMS} = 0.130, \text{ } n = 45 \text{ (MLR)}$$

$$\begin{aligned} \lg H_{50} = & 0.9872 + 0.0883X_3 - 0.0032X_4 + 0.0231X_5 + 0.0374X_6 \\ & + 0.1007X_7 - 0.0698X_9 + 0.4096X_{10} + 0.01984X_{13} \\ & - 0.0103X_{15} + 0.0031X_{16} \end{aligned} \quad (19)$$

$$R^2 = 0.8417, \text{ RMS} = 0.134, \text{ } n = 45 \text{ (PLS)}$$

$$\begin{aligned} \lg H_{50} = & 1.8551 + 0.2131X_3 + 0.0213X_4 - 0.1587X_5 - 0.4283X_6 \\ & + 0.0168X_7 - 0.0936X_8 - 0.0810X_9 + 0.1197X_{10} \\ & + 0.0062X_{12} - 0.0027X_{13} - 0.0547X_{14} + 0.0226X_{15} \\ & - 0.0234X_{16} \end{aligned} \quad (20)$$

$$R^2 = 0.8010, \text{ RMS} = 0.200, \text{ } n = 43 \text{ (MLR)}$$

$$\begin{aligned} \lg H_{50} = & 1.5312 + 0.2352X_3 + 0.0107X_4 - 0.1438X_5 - 0.1964X_6 \\ & + 0.0445X_7 - 0.0649X_8 - 0.0570X_9 + 0.1546X_{10} \\ & + 0.0210X_{12} - 0.0039X_{13} - 0.0156X_{14} + 0.0192X_{15} \\ & - 0.0048X_{16} \end{aligned} \quad (21)$$

$$R^2 = 0.7815, \text{ RMS} = 0.209, \text{ } n = 43 \text{ (PLS)}$$

Table 2
Experimental and predicted H_{50} by BPNN, MLR, PLS and other methods.

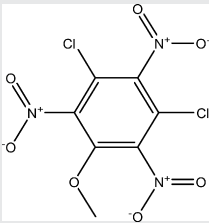
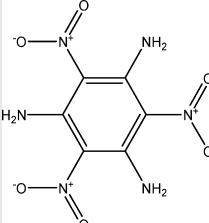
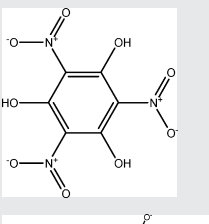
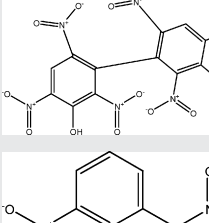
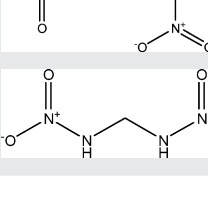

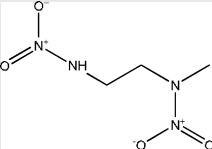
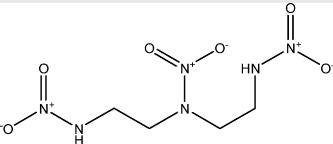
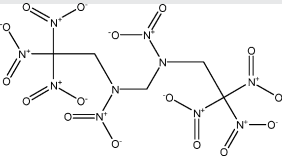
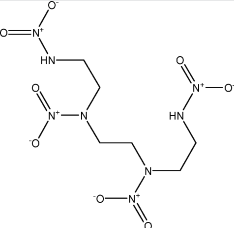
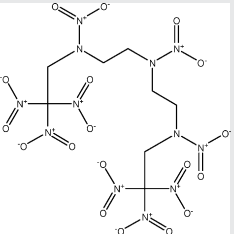
Number	Compounds	Structure	Exp. H_{50} (cm)	Predicted H_{50} (cm)				
				MLR	PLS	BPNN	Nefati et al. [21]	Keshavarz and Jaafari [23]
1	1-Methoxy-3,5-dichloro-2,4,6-trinitrobenzene*		75	72.28	71.94	76.2	57.11	-
2	1,3,5-Triamino-2,4,6-trinitrobenzene*		490	352.37	368.13	477.5	236.32	337
3	2,4,6-Trinitrophenol		27	62.95	62.52	32.4	49.39	-
4	3,3'-Dihydroxy-2,2',4,4',6,6'-hexanitrobiphenyl		40	48.75	48.53	36.2	47.14	56
5	1-Dinitromethyl-3-nitrobenzene		105	153.82	148.94	108.9	73.23	112
6	<i>N,N'</i> -Dinitro-methanediamine		13	32.36	32.36	24.4	36.39	9

Table 2 (Continued)

Number	Compounds	Structure	Exp. H_{50} (cm)	Predicted H_{50} (cm)				
				MLR	PLS	BPNN	Nefati et al. [21]	Keshavarz and Jaafari [23]
7	<i>N</i> -Methyl- <i>N,N'</i> -dinitro-1,2-ethanediamide		114	52.84	53.33	93.1	87.50	–
8	<i>N,N'</i> -Dinitro- <i>N</i> -[2-(nitroamino)ethyl]-1,2-ethanediamine		39	25	28.12	27.2	33.66	49
9	<i>N,N'</i> -bis-(2,2,2-Trinitroethyl)- <i>N,N'</i> -dinitromethanediamine		5	5.51	5.38	4.7	7.61	10
10	<i>N,N'</i> -dinitro- <i>N,N'</i> -bis-[2-nitroamino-ethyl]-1,2-ethanediamine		53	31.77	35.73	54.2	36.91	73
11	1,1,1,3,6,9,11,11,11-Nonanitro-3,6,9-triazaundecane		12	7.29	6.98	11.3	15.42	5

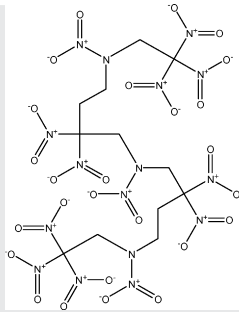
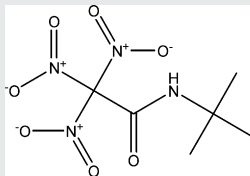
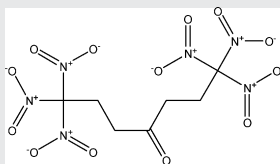
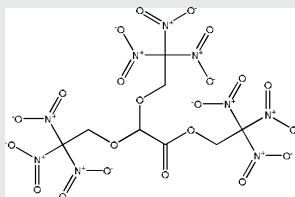
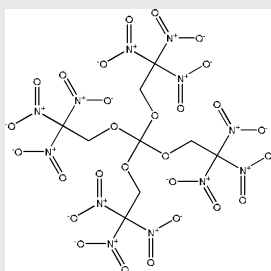
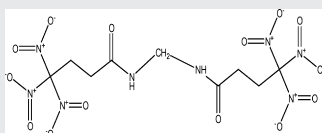
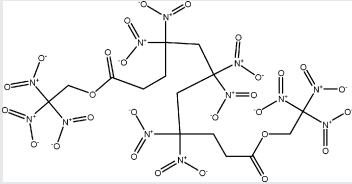
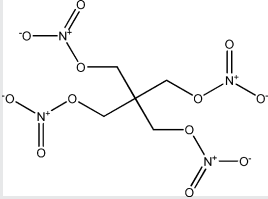
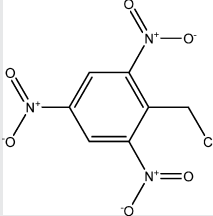
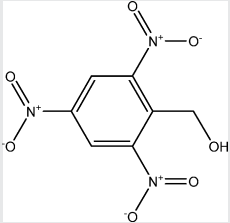
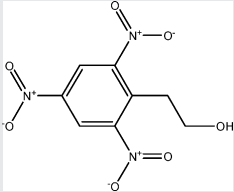
12	1,1,1,3,6,6,8,10,10,13,15,15,15-Tridecanitro-3,8,13-triazapentadecane		23	10.94	10.23	24.8	17.98	7
13	N-(<i>t</i> -Buty)-trinitroacetamide		110	236.05	232.81	117.5	191.56	168
14	1,1,1,7,7,7-Hexanitroheptanone-4		34	14	22.18	30.5	30.80	35
15	Trinitroethyl-bis-(trinitroethoxy)-acetate		6	7.59	7.74	6.1	11.21	9
16	Tetrakis-(2,2,2,-trinitroethyl)-orthocarbonate		7	3.95	4.27	7.4	7.91	10
17	Methylene-bis-(4,4,4-trinitrobutyramide)		113	51.4	43.75	85.5	72.29	58

Table 2 (Continued)

Number	Compounds	Structure	Exp. H_{50} (cm)	Predicted H_{50} (cm)				
				MLR	PLS	BPNN	Nefati et al. [21]	Keshavarz and Jaafari [23]
18	bis-(2,2,2-Trinitroethyl)-4,4,6,6,8,8-hexanitro-undecanedioate		32	45.08	41.21	30.1	35.47	46
19	2,2-bis-(Nitroxymethyl)-1,3-propanediol dinitrate		13	31.33	34.2	13.2	13.07	52
20	2,4,6-Trinitrobenzyl chloride*		44	47.32	46.56	44.8	63.20	–
21	2,4,6-Trinitrobenzyl alcohol*		52	59.43	60.12	61.7	74.39	–
22	1-Hydroxyethyl-2,4,6-trinitrobenzene*		68	62.81	64.57	64	114.55	–

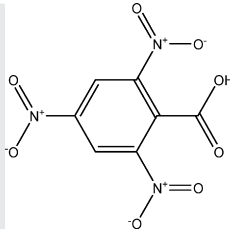
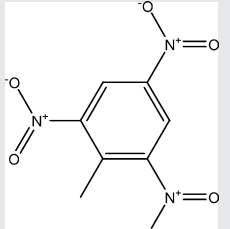
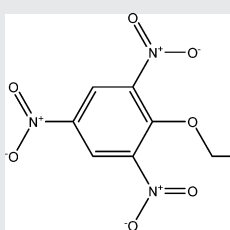
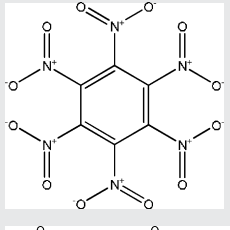
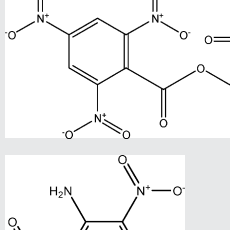
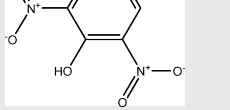
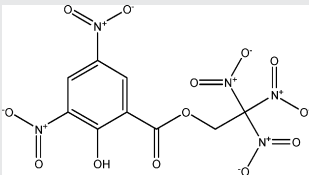
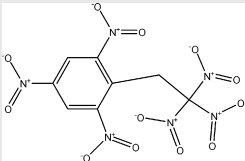
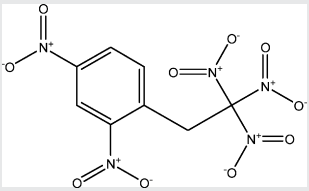
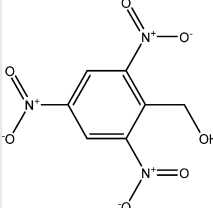
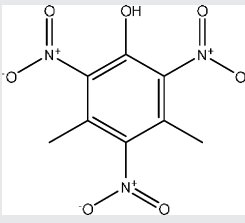
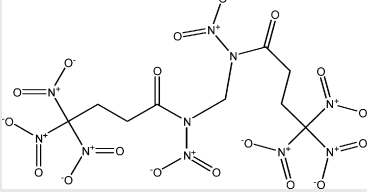
23	2,4,6-Trinitrobenzoic acid*		109	55.08	54.08	74	78.58	102
24	2,4,6-Trinitrotoluene*		160	115.35	116.68	175.8	98.06	112
25	1-Ethoxy-2,4,6-trinitrobenzene*		190	102.33	106.41	125.6	213.85	-
26	Hexanitro benzene		12	10.84	9.66	13	14.79	-
27	2',2'-Trinitroethyl-2,4,6-trinitrobenzoate		24	22.75	22.39	21.2	23.63	27
28	2,4,6-Trinitro-3-amino-phenol		138	93.54	93.97	98.9	136.71	122

Table 2 (Continued)

Number	Compounds	Structure	Exp. H_{50} (cm)	Predicted H_{50} (cm)				
				MLR	PLS	BPNN	Nefati et al. [21]	Keshavarz and Jaafari [23]
29	2',2',2'-Trinitroethyl-3,5-dinitrosalicylate		45	80.35	82.41	68.4	68.52	71
30	1-(2,2,2-Trinitroethyl)-2,4,6-trinitrobenzene		13	16.94	17.06	13.9	17.61	19
31	1-(2,2,2-Trinitroethyl)-2,4-dinitrobenzene		31	57.68	60.12	34.6	27.91	32
32	2,4,6-Trinitrobenzylalcohol		52	59.43	60.12	61.7	74.39	93
33	3,5-Dinitro-2,4,6-trinitrophenol		77	112.72	114.55	114.3	68.85	184
34	<i>N,N'</i> -Dinitromethylene-bis-(4,4,4-trinitro)-butyramide		13	22.13	20.99	19.4	14.89	21

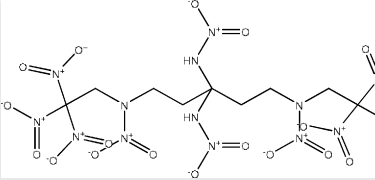
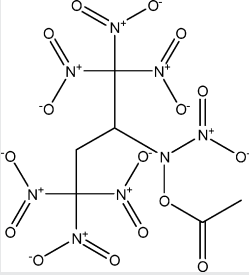
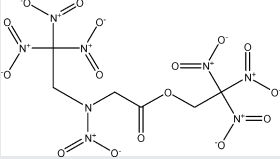
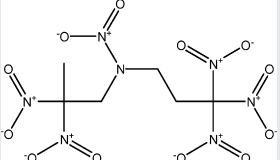
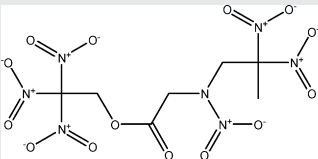
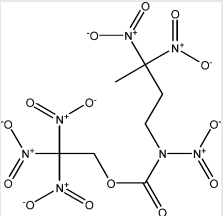
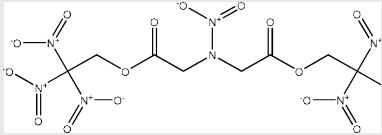
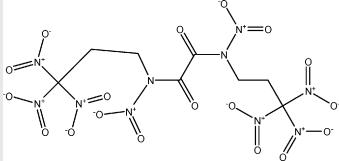
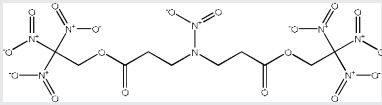
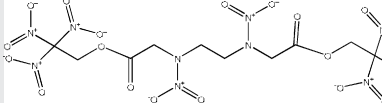
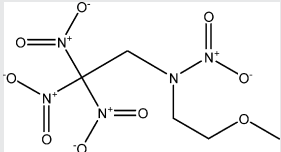
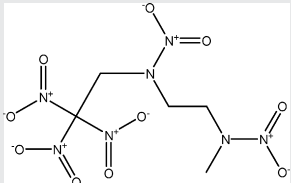
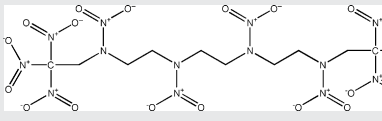
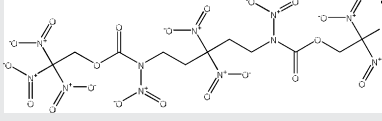
35	bis-(5,5,5-Trinitro-3-nitrazapentanyl)-methylenedinitramine		15	15.1	16.6	14.9	11.12	4
36	2,2,2-Trinitroethyl-N-(2,2,2-trinitroethyl)-nitramino acetate		9	11.67	11.35	9.4	11.05	11
37	2,2,2-Trinitroethyl-4-nitrazavalerate		35	41.59	41.21	55.1	25.01	114
38	Trinitropropyl-(2,2-dinitropropyl)-nitramine		17	25.64	26.55	21.3	24.89	16
39	Trinitroethyl-5,5-dinitro-3-nitrazahexanoate		25	30.13	29.92	24.3	23.98	20
40	2,2,2-Trinitroethyl-2,5,5-trinitro-2-azahexanoate		22	39.54	41.88	28.9	23.98	20

Table 2 (Continued)

Number	Compounds	Structure	Exp. H_{50} (cm)	Predicted H_{50} (cm)				
				MLR	PLS	BPNN	Nefati et al. [21]	Keshavarz and Jaafari [23]
41	bis-(2,2,2-Trinitroethyl)-3-nitrazaglutarate		14	23.28	21.68	18.8	16.04	0
42	<i>N,N'</i> -Dinitro- <i>N,N'</i> -bis-(3,3,3-trinitropropyl)-oxamide		9	15.21	15.31	8.7	10.88	24
43	bis-(2,2,2-Trinitroethyl)-4-nitraza-1,7-heptanedioate		29	29.99	27.61	29.6	31.05	41
44	bis-(2,2,2-Trinitroethyl)-3,6-dinitraza-1,8-octanedioate		29	22.44	21.38	20.4	20.33	17
45	Trinitroethyl-2-methoxy-ethylnitramine		42	32.81	33.5	30.6	43.77	30
46	<i>N</i> -Methyl- <i>N'</i> -trinitroethyl- <i>N,N'</i> -dinitro-1,2-ethanediamine		11	25.41	25.82	17.6	23.40	21
47	1,1,1,3,6,9,12,14,14,14-Decanitro-3,6,9,12-tetraza-tetradecane		19	9.53	9.66	19.7	21.25	18
48	bis-trinitroethyl-5,5-dinitro-2,8-dinitraza-nonanedioate		12	18.32	18.71	13.5	16.20	7

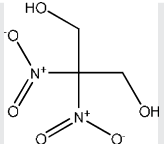
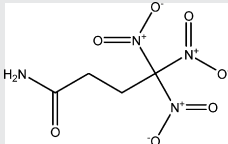
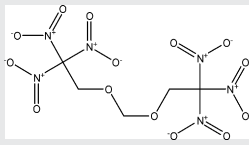
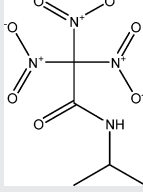
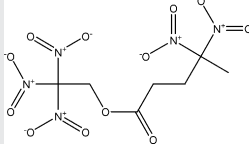
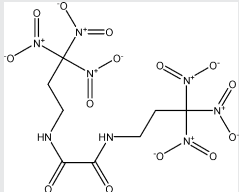
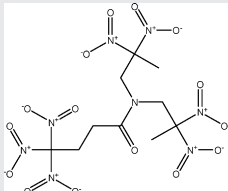
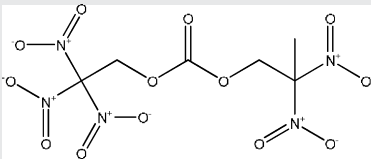
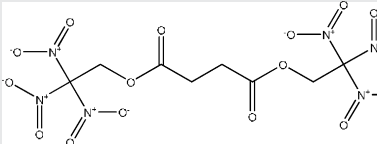
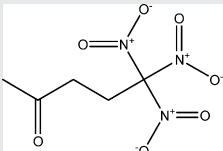
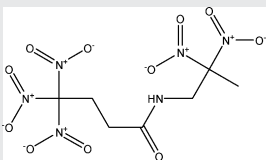
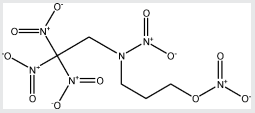
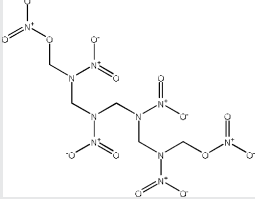
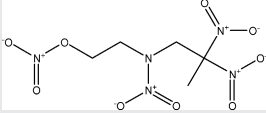
49	2,2-Dinitro-1,3-propane diol		110	49.89	49.66	82.2	101.30	107
50	4,4,4-Trinitrobutyramide		40	56.36	49.77	67.9	40.71	41
51	bis-(Trinitroethoxy)-methane		17	14.32	14.93	11.4	18.33	14
52	<i>N</i> -(2-Propyl)-trinitroacetamide		112	96.61	93.54	108.4	121.34	90
53	2,2,2-Trinitroethyl-4,4-dinitrovalerate		70	41.78	40.46	39.5	52.05	89
54	<i>N,N'</i> -bis-(3,3,3-trinitropropyl)-oxamide		45	38.46	35.56	56	48.66	29
55	<i>N,N</i> -bis-(2,2-Dinitropropyl)-4,4,4-trinitrobutyramide		72	52	51.17	48.8	75.81	87

Table 2 (Continued)

Number	Compounds	Structure	Exp. H_{50} (cm)	Predicted H_{50} (cm)				
				MLR	PLS	BPNN	Nefati et al. [21]	Keshavarz and Jaafari [23]
56	Trinitroethyl-2,2-dinitropropylcarbonate		15	33.34	34.67	28.9	31.26	25
57	bis-(2,2,2-Trinitroethyl)-succinate		30	28.64	25.41	24.4	29.35	41
58	5,5,5-Trinitropentanone-2		125	48.53	40.83	65.8	96.76	73
59	2,2-Dinitropropyl-4,4,4-trinitrobutyramide		72	55.59	53.21	56.4	68.38	73
60	3-[N-(2,2,2-Trinitroethyl)-nitramino]-propylnitrate		12	15.1	15.56	10.7	19.46	8
61	1,9-Dinitrato-2,4,6,8-tetranitrazanonane		10	16.9	16.87	11	11.87	10
62	3,5,5-Trinitro-3-azahexyl-nitrate		21	35.65	37.24	34.4	32.38	59

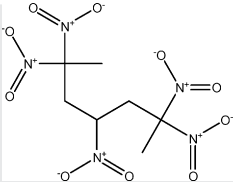
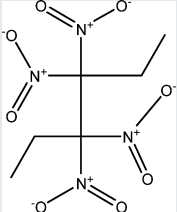
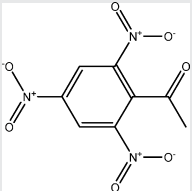
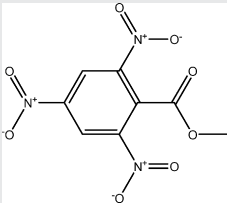
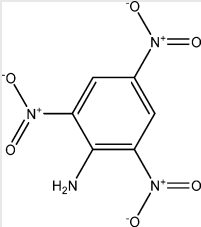
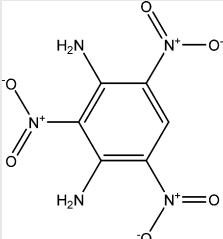
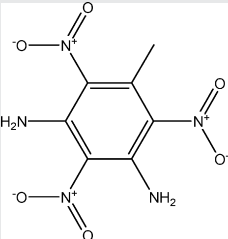
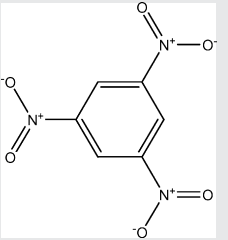
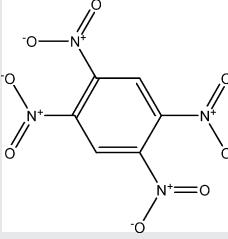
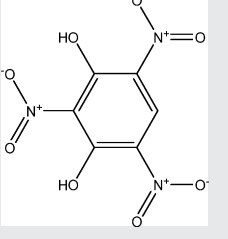
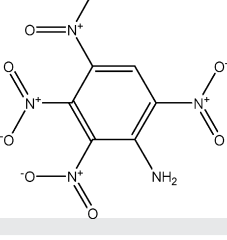
63	2,2,4,6,6-Pentanitroheptane		56	48.98	50.93	56.6	87.30	80
64	3,3,4,4-Tetranitro-hexane		80	73.45	76.38	83.4	22.92	117
65	2,4,6-Trinitro-acetylbenzene*		79	96.83	84.72	133.4	144.11	-
66	Methyl-2,4,6-trinitrobenzoate*		90	91.62	83.56	119.1	129.84	-
67	2,4,6-Trinitroaniline*		177	100.93	101.16	109.9	136.46	172
68	1,3-Diamino-2,4,6-trinitrobenzene*		320	187.93	187.93	218.3	178.24	290

Table 2 (Continued)

Number	Compounds	Structure	Exp. H_{50} (cm)	Predicted H_{50} (cm)				
				MLR	PLS	BPNN	Nefati et al. [21]	Keshavarz and Jaafari [23]
69	1-Methyl-3,5-diamino-2,4,6-trinitrobenzene**		239	347.54	348.34	462.4	151.18	-
70	1,3,5-Trinitrobenzene*		100	61.24	61.24	63.8	106.24	108
71	1,2,4,5-Tetranitrobenzene		27	23.6	23.5	20.7	113.66	24
72	2,4,6-Trinitroresorcinol		43	47.97	48.31	40	60.84	79
73	2,3,4,6-Tetranitroaniline		41	51.4	50.82	44.2	68.05	50

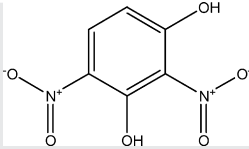
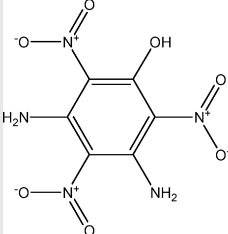
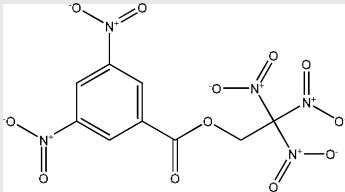
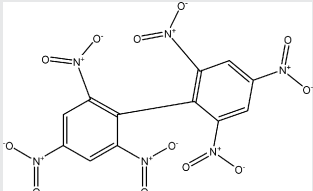
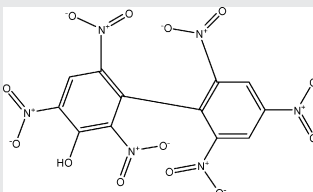
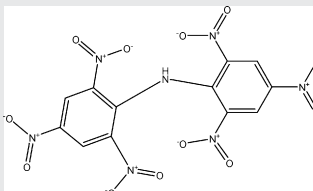
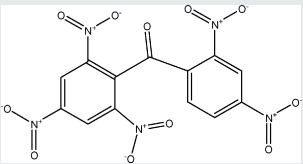
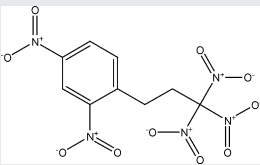
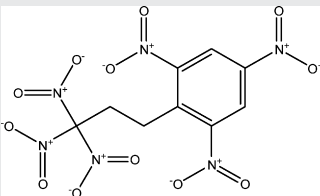
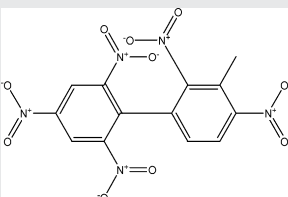
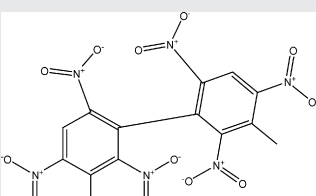
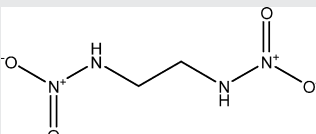
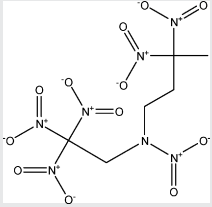
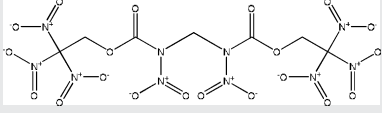
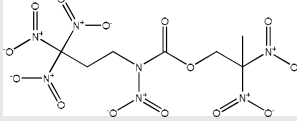
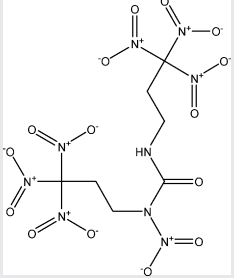
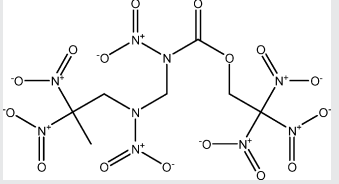
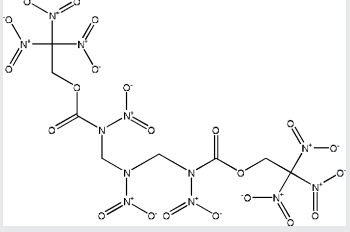
74	2,4-Dinitroresorcinol		296	92.47	93.33	108.1	138.45	227
75	1-Hydroxy-3,5-diamino-2,4,6-trinitrobenzene		120	184.93	187.93	197.7	133.05	186
76	2',2',2'-Trinitroethyl-3,5-dinitrobenzoate		73	48.31	47.1	35.9	37.62	83
77	2,2',4,4',6,6'-Hexanitrobiphenyl		85	35.32	36.39	29.3	55.49	55
78	3-Hydroxy-2,2',4,4',6,6'-hexanitrobiphenyl		42	39.54	40.18	35.3	49.14	59
79	2,2',4,4',6,6'-Hexanitrodiphenylamine		48	49.66	53.09	29.7	77.43	62

Table 2 (Continued)

Number	Compounds	Structure	Exp. H_{50} (cm)	Predicted H_{50} (cm)				
				MLR	PLS	BPNN	Nefati et al. [21]	Keshavarz and Jaafari [23]
80	2,2',4,4',6-Pentanitrobenzophenone		54	142.56	132.13	104.5	68.80	79
81	1-(3,3,3-Trinitropropyl)-2,4-dinitrobenzene		31	35.89	36.9	23.2	41.96	72
82	1-(3,3,3-Trinitropropyl)-2,4,6-trinitrobenzene		21	24.38	24.89	18.7	26.71	22
83	3-Methyl-2,2',4,4',6'-pentanitrobiphenyl		143	140.28	148.25	105.9	82.36	93
84	3,3'-Dimethyl-2,2',4,4',6,6'-hexanitrobiphenyl		135	96.16	98.86	87.1	46.46	71
85	<i>N,N'</i> -Dinitro-1,2-ethanediamine		34	35.08	35.81	25.6	54.88	15

86	Cyclotrimethylene-trinitramine		26	22.23	22.23	41.5	22.17	31
87	bis-(2,2,2-Trinitroethyl)-nitramine		5	5.43	5.33	3.8	7.50	1
88	<i>N,N'</i> -dimethyl- <i>N,N'</i> -dinitrooxamide		79	66.68	57.41	151	37.84	93
89	1,3,3,5,5-Pentanitropiperidine		14	30.06	30.55	25.9	20.45	17
90	2,2,2-Trinitroethyl-3',3',3'-trinitropropyl-nitramine		6	8.2	8.07	6.7	11.13	10
91	<i>N,N'</i> -3,3-Tetranitro-1,5-pentanediamine		35	57.54	58.75	62.8	38.12	23
92	<i>N</i> -Nitro- <i>N</i> -(3,3,3-trinitropropyl)-2,2,2-trinitroethyl-carbamate		9	11.61	11.8	8.6	11.05	11

Table 2 (Continued)

Number	Compounds	Structure	Exp. H_{50} (cm)	Predicted H_{50} (cm)				
				MLR	PLS	BPNN	Nefati et al. [21]	Keshavarz and Jaafari [23]
93	2,2,2-Trinitroethyl-3,3-dinitrobutyl-nitramine		20	20.56	21.23	16.1	24.89	16
94	bis-(Trinitroethyl)-2,4-dinitrazapentanedioate		10	10.02	10.52	5.1	8.05	24
95	2,2-Dinitropropyl-5,5,5-trinitro-2-nitrazapentanoate		16	28.97	29.44	20.5	23.98	20
96	N-Nitro-N,N'-bis-(trinitropropyl)-urea		21	17.7	17.3	13.7	19.49	9
97	2,2,2-Trinitroethyl-2,4,6,6-tetranitro-2,4-diazaheptanedioate		18	19.63	20.46	10.9	15.11	3
98	bis-(Trinitroethyl)-2,4,6-trinitraza-heptanedioate		13	8.93	9.38	5.2	9.00	22

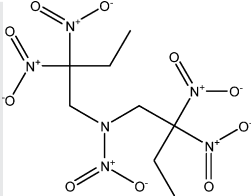
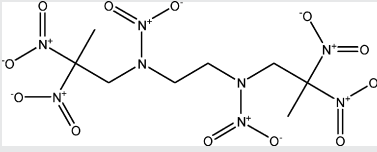
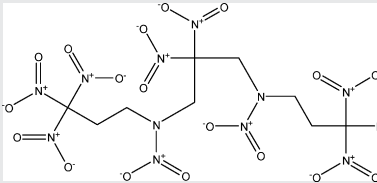
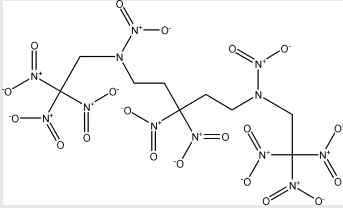
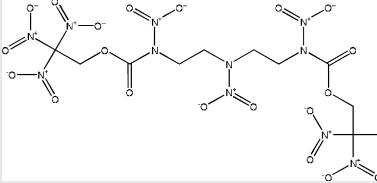
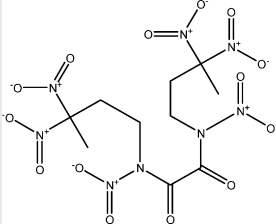
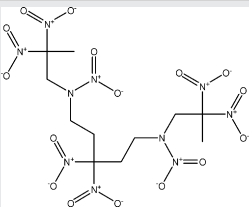
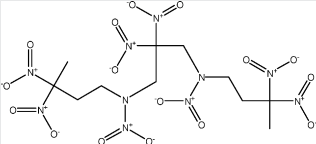
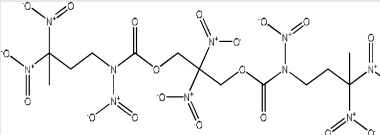
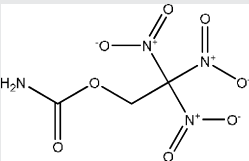
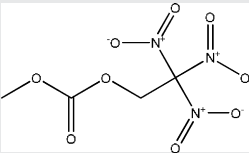
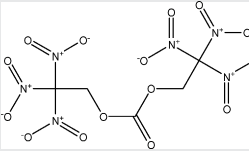
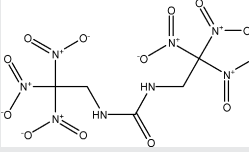
99	<i>N</i> -(2,2-Dinitrobutyl)- <i>N</i> ,2,2-trinitro-1-butanamine		80	110.92	116.14	89.7	85.17	90
100	2,2,4,7,9,9-Hexanitro-4,7-diazadecane		72	49.32	53.58	43	38.85	30
101	1,1,1,4,6,6,8,11,11,11-Decanitro-4,8-diazaundecane		11	11.22	10.94	17.9	15.09	5
102	1,1,1,3,6,6,9,11,11,11-Decanitro-3,9-diazaundecane		10	9.91	9.77	15.6	15.09	5
103	bis-(2,2,2-Trinitroethyl)-2,5,8-trinitraza nonanedioate		17	16.63	16.71	13.6	16.46	8
104	<i>N,N'</i> -Dinitro- <i>N,N'</i> -bis-(3,3-dinitrobutyl)-oxamide		37	70.96	72.44	43.3	36.68	51

Table 2 (Continued)

Number	Compounds	Structure	Exp. H_{50} (cm)	Predicted H_{50} (cm)				
				MLR	PLS	BPNN	Nefati et al. [21]	Keshavarz and Jaafari [23]
105	2,2,4,7,7,10,12,12-Octanitro-4,10-diazatridecane		44	60.95	66.53	61.5	44.49	36
106	2,2,5,7,7,9,12,12-Octanitro-5,9-diazatridecane		37	69.02	74.47	66.2	44.49	36
107	2,2-Dinitropropanediol-bis-(5,5-dinitro-2-nitroaza-hexanoate)		138	140.93	148.25	48.8	43.34	113
108	2,2,2-Trinitroethyl-carbamate		18	49.09	46.24	55.5	44.19	10
109	Methyl-2,2,2-trinitroethyl carbonate		28	39.9	37.84	43.9	45.73	27
110	bis-(2,2,2-Trinitroethyl)-carbonate		16	12.27	12.79	10.3	12.44	10
111	<i>N,N'</i> -bis-(2,2,2-trinitroethyl)-urea		17	16.87	16.9	19.4	21.14	12

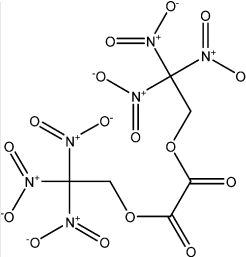
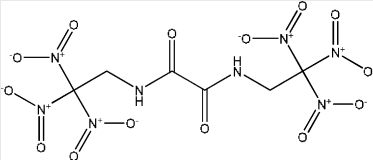
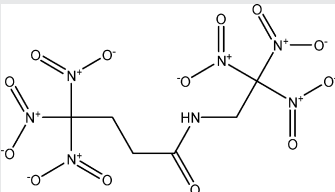
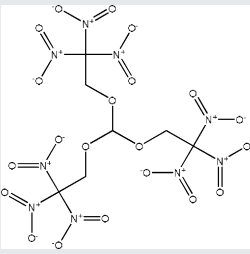
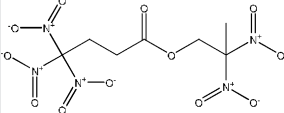
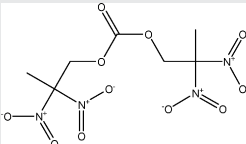
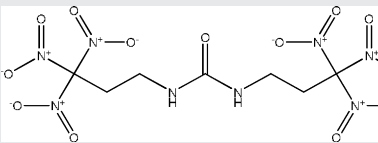
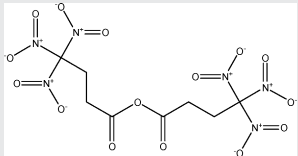
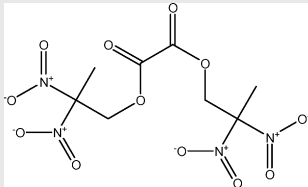
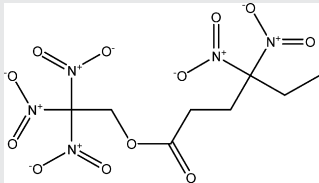
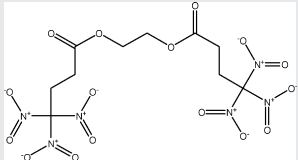
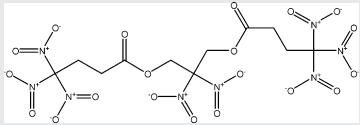
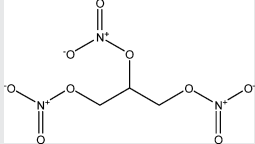
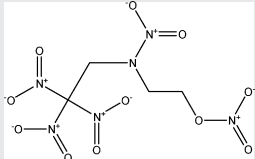
112	bis-(trinitroethyl)-oxalate		15	15.63	16.41	14.2	12.74	14
113	bis-(Trinitroethyl)-oxamide		13	20.42	20.18	23.3	23.65	21
114	N-Trinitroethyl-4,4,4-trinitrobutyramide		18	21.73	20.65	20.4	25.69	11
115	tris-(2,2,2-trinitroethyl)-orthoformate		7	6.05	6.22	5.5	10.74	10
116	2,2-Dinitropropyl-trinitrobutyrate		151	46.34	44.87	44.7	52.05	89
117	bis-(2,2-Dinitropropyl)-carbonate		300	90.57	93.97	86.7	81.60	191
118	bis-(Trinitropropyl)-urea		23	30.2	29.44	47.1	50.27	23

Table 2 (Continued)

Number	Compounds	Structure	Exp. H_{50} (cm)	Predicted H_{50} (cm)				
				MLR	PLS	BPNN	Nefati et al. [21]	Keshavarz and Jaafari [23]
119	4,4,4-Trinitrobutyricanhydride		30	30.76	27.67	30.6	29.53	40
120	bis-(2,2-Dinitropropyl)-oxalate		227	108.64	109.65	122.2	84.08	183
121	2,2,2-Trinitroethyl-4,4-dinitrohexanoate		138	62.52	59.57	60.3	77.13	146
122	Ethylene-bis-(4,4,4-trinitrobutyrate)		120	41.69	35.97	34.4	61.93	121
123	2,2-Dinitropropane-1,3-diol-bis-(4,4,4-trinitrobutyrate)		50	43.45	40.27	44.6	37.88	61
124	1,2,3-Propanetrioltrinitrate		20	20.75	20.89	13.3	16.65	10
125	N-(2,2,2-Trinitroethyl)-nitraminoethyl nitrate		7	14.16	14.32	9.6	13.90	10

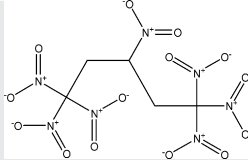
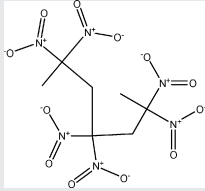
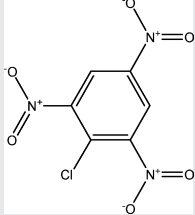
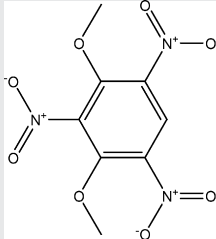
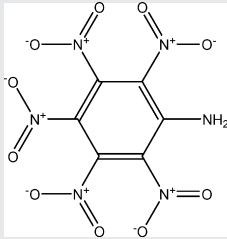
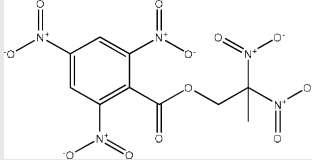
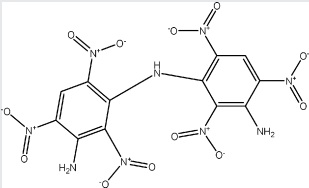
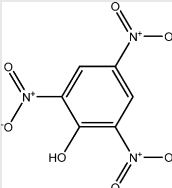
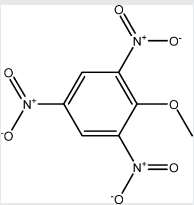
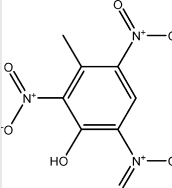
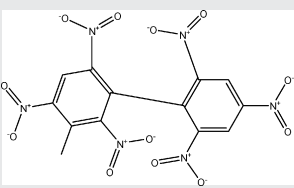
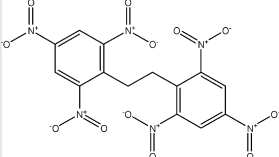
126	1,1,1,3,5,5,5-Heptanitropentane		8	6.14	5.81	5.2	9.17	16
127	2,2,4,4,6,6-Hexanitroheptane		29	32.36	34.91	30.6	48.19	43
128	2,4,6-Trinitro-1-chlorobenzene*		79	41.3	40.36	40.6	65.19	-
129	1,3-Dimethoxy-2,4,6-trinitrobenzene*		251	120.5	125.6	116.4	161.85	284
130	2,3,4,5,6-Pentanitroaniline		15	39.9	37.15	35.9	33.22	14
131	2',2'-Dinitropropyl-2,4,6-trinitrobenzoate		214	66.37	65.77	62.1	70.65	156

Table 2 (Continued)

Number	Compounds	Structure	Exp. H_{50} (cm)	Predicted H_{50} (cm)				
				MLR	PLS	BPNN	Nefati et al. [21]	Keshavarz and Jaafari [23]
132	3,3'-Diamino-2,2',4,4',6,6'-hexanitrodiphenylamine		132	255.86	267.3	148.3	104.47	102
133	Picric acid**		87	47.21	47.53	49.7	78.32	–
134	2,4,6-Trinitroanisole*		192	85.11	86.3	100.2	131.10	216
135	2,4,6-Trinitro-m-cresol		191	73.79	74.82	87.9	74.39	93
136	3-Methyl-2,2',4,4',6,6'-hexanitrobiphenyl		53	52.72	54.33	48.8	50.87	53
137	2,2',4,4',6,6'-Hexanitrobibenzyl		114	74.82	80.17	45.2	46.46	80

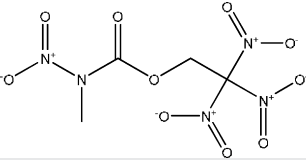
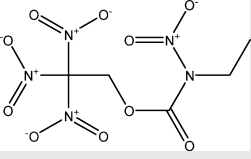
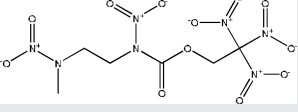
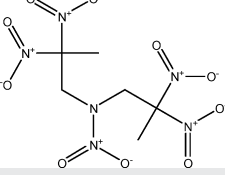
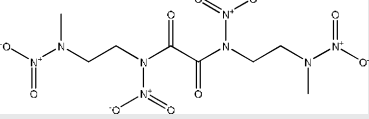
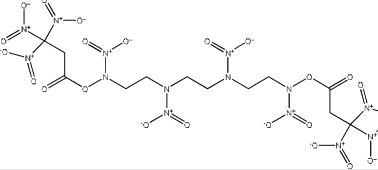
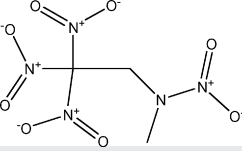
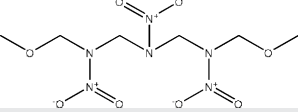
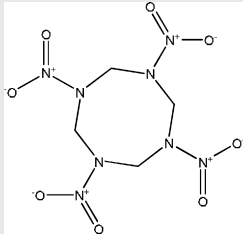
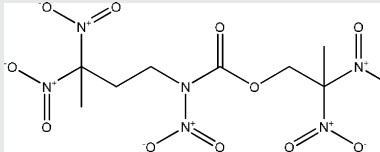
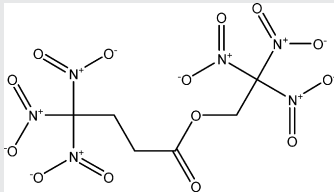
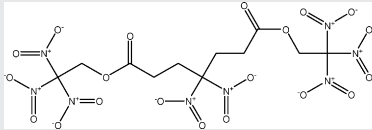
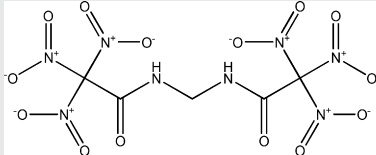
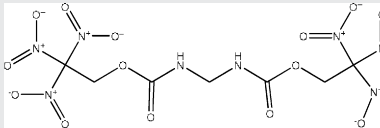
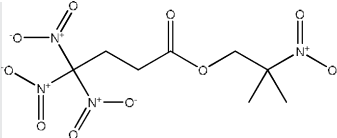
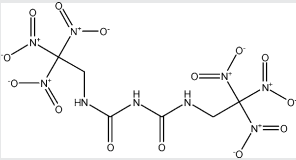
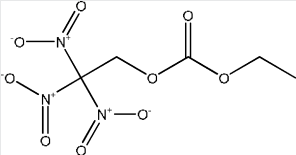
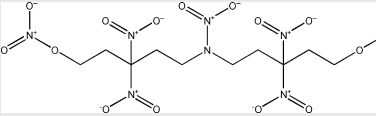
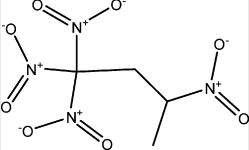
138	<i>N</i> -Methyl- <i>N</i> -nitro-(trinitroethyl)-carbamate		17	24.77	24.1	22.8	21.43	10
139	Trinitroethyl- <i>N</i> -ethyl- <i>N</i> -nitro-carbamate		19	38.28	36.81	37.9	30.85	26
140	2',2',2'-Trinitroethyl-2,5-dinitrazahexanoate		15	31.77	31.62	29.3	22.30	30
141	<i>N</i> -(2,2-dinitropropyl)- <i>N</i> ,2,2-trinitro-1-propanamine		29	41.3	44.06	35	41.07	31
142	<i>N,N'</i> -Dinitro- <i>N,N'</i> -bis-(3-nitrazabutyl)-oxamide		90	97.27	89.74	138.7	33.78	143
143	1,1,1,18,18,18-Hexanitro-3,16-dioxa-4,15-dioxo-5,8,11,14-tetranitrazaoctadecane		19	18.62	18.88	20.1	22.69	17
144	Methyl-2,2,2-trinitroethylnitramine		9	18.92	18.92	19.1	24.08	10
145	1,7-dimethoxy-2,4,6-trinitrazaheptane		166	102.09	106.91	146.9	54.23	169

Table 2 (Continued)

Number	Compounds	Structure	Exp. H_{50} (cm)	Predicted H_{50} (cm)				
				MLR	PLS	BPNN	Nefati et al. [21]	Keshavarz and Jaafari [23]
146	Cyclotetramethylene-tetranitramine		29	23.6	23.66	29.9	18.23	31
147	2,2,6,9,9-Pentanitro-4-oxa-5-oxo-6-azadecane		47	77.8	78.89	60.3	53.78	60
148	2,2,2-Trinitroethyl-4,4,4-trinitrobutyrate		18	16.83	16.14	15.6	20.15	18
149	bis-(2,2,2-Trinitroethyl)-4,4-dinitroheptanedioate		68	40.27	37.07	40.9	37.88	61
150	Methylene-bis- <i>N,N'</i> -(2,2,2-trinitroacetamide)		9	9.38	10.3	9.6	13.72	9
151	Methylene-bis-(trinitroethyl)-carbamate		27	24.15	25	26.6	31.86	12

152	Nitroisobutyl-4,4,4-trinitrobutyrate		279	142.89	133.97	123	144.05	299
153	1,5-bis-(Trinitroethyl)-biuret		24	25.64	25.06	42.6	26.74	10
154	Ethyl-2,2,2-trinitroethylcarbonate		81	56.62	53.33	61.7	70.19	142
155	4,4,8,8-Tetranitro-1,11-dinitro-6-nitrazoundecane		87	42.36	45.08	40.4	30.63	63
156	1,1,1,3-Tetranitrobutane		33	25.18	25	30.5	34.08	36

The substances from 1 to 64 composed the training samples, those from 65 to 127 were the validation samples, and those from 128 to 156 were the prediction samples. The compounds marked (*) were taken from literature [4], the ones marked (**) were taken from literature [3], and the others from literature [32].

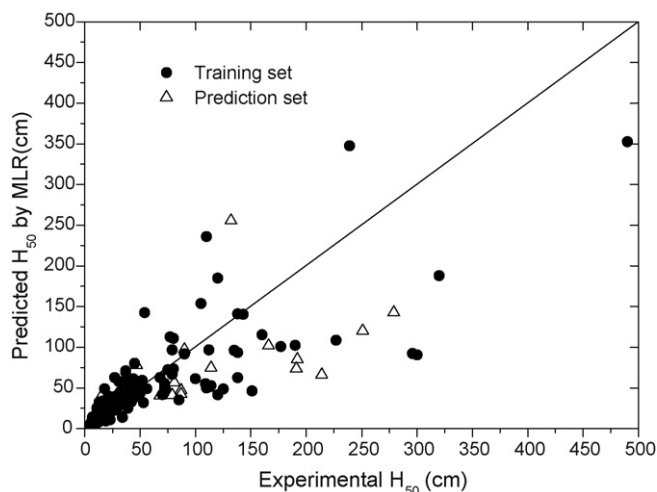


Fig. 2. Correlation between the predicted and experimental H_{50} by MLR.

Eqs. (16) and (17) are the regression results for nitroaromatic compounds, Eqs. (18) and (19) are for nitramine compounds, and Eqs. (20) and (21) are for nitroaliphatic compounds.

The obtained equations are then used to predict the impact sensitivity values of the compounds in the prediction sets for external validation, respectively. Finally, the predicted impact sensitivity values for each dataset are obtained, and the main performance parameters of these models are shown in Table 4.

From Table 4, it can be seen that the model for nitramine compounds perform better than those for other two classes of compounds, as it showed larger correlation coefficients (R^2 and R_{ext}^2), lower RMS, as well as better robustness (Q_{ext}^2) for both training and prediction sets. As for the class of nitroaromatic compounds, although the obtained models got good results for training set, the predicted results were poor. The reasons for the weak predictive ability of this model may be attributed to the low ratio of samples to descriptors (39/15). Moreover, the unreasonable division of the dataset may also lead to the poor predictive ability of the developed model. As for the class of nitroaliphatic compounds, the results for prediction set were unreasonably much better than those for training set. This phenomena may result from the chance correlation problems.

For BPNN modeling, as discussed above, a 16–12–1 architecture was applied as the final network. We repeated the training procedure 10 times and recorded the result of each time, and then an average value was taken as finally prediction result of each compound. The predicted impact sensitivity values for all 156 compounds are obtained and presented in Table 2. The main performance parameters of ANN model are shown in Table 3. A plot of the predicted impact sensitivity values versus the experimental ones for ANN model is shown in Fig. 4.

As can be seen from Table 3, both the MLR and PLS models showed poor abilities for external prediction, which would prove that, there is not a simple linear correlation between the ETSI and

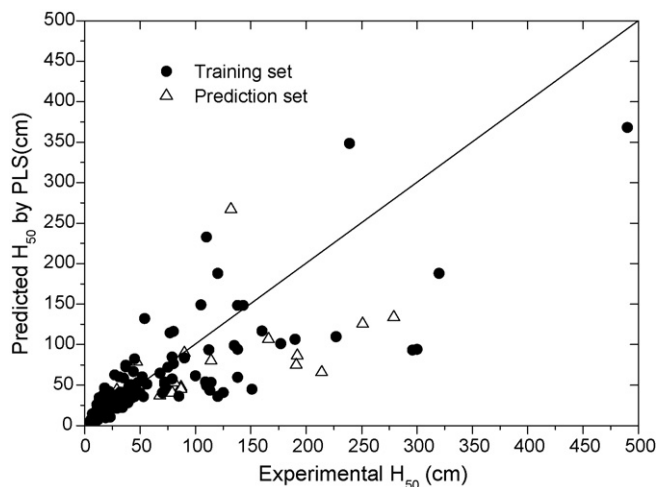


Fig. 3. Correlation between the predicted and experimental H_{50} by PLS.

impact sensitivity. Meanwhile, the non-linear BPNN model can give better results here with higher correlation coefficients (R^2 and R_{ext}^2), lower RMS, as well as better robustness (Q_{ext}^2) in both training set and prediction set, which indicated that the BPNN method not only performed well in model development, but also had superior prediction ability than the linear ones. This fact proved our previous conjecture that a non-linear correlation may exist between the ETSI and impact sensitivity.

Besides, a Y-scrambling [36] was also executed to ensure the robustness of the BPNN model, in which the dependent variables were scrambled of random numbers. The trials were repeated 10 times, and for each time, very small coefficients for both model fitting and validation were achieved. It can be thus concluded that only the correct dependent variable can be used to generate reasonable models, and the chance correlation had little or no effect in the presented model.

Moreover, it would be worthwhile to compare our present work with those previous ones. Nefati et al. [21] first introduced the BPNN method to the QSPR study of impact sensitivity. In their study, they tried several combinations of molecular descriptors, and built models with the same three modeling methods as that were employed in our study. However, direct comparison of the results cannot be performed between the work of Nefati et al. and the presented one, because the dataset and descriptors employed in these two studies were different. So, in order to make a direct comparison, we employed the descriptors used in the work of Nefati et al. to build a new BPNN model by using the current dataset. The obtained results were shown in Table 3 and corresponding predicted values were listed in Table 2. As can be seen, the results of the new BPNN model were a little worse than those of our presented model for both the training and prediction sets. Moreover, it must be noted that for the work of Nefati et al., the external validation was not carried out, thus the true prediction ability of the model for new organic compounds which were not used for model development was not clear, although this work showed a better fitting results than ours.

Table 3
Performance comparison between models obtained by MLR, PLS, BPNN and other method.

Model	Training set			Prediction set		
	R^2	Q_{LOO}^2	RMS	R_{ext}^2	Q_{ext}^2	RMS
MLR	0.771	0.593	0.212	0.715	0.716	0.251
PLS	0.766	0.674	0.214	0.718	0.718	0.250
BPNN	0.816	–	0.192	0.740	0.738	0.247
Nefati et al. [21]	0.795	–	0.203	0.756	0.703	0.257

Table 4
Performance of MLR and PLS models for three classes of nitro compounds.

Classes	Model	Training set			Prediction set		
		R^2	Q_{100}^2	RMS	R_{ext}^2	Q_{ext}^2	RMS
Nitroaromatics	MLR	0.840	0.529	0.148	0.457	0.522	0.267
	PLS	0.835	0.565	0.150	0.424	0.497	0.277
Nitramine	MLR	0.852	0.695	0.130	0.856	0.670	0.225
	PLS	0.842	0.724	0.134	0.864	0.676	0.223
Nitroaliphatics	MLR	0.801	0.512	0.200	0.932	0.811	0.188
	PLS	0.782	0.484	0.209	0.974	0.837	0.175

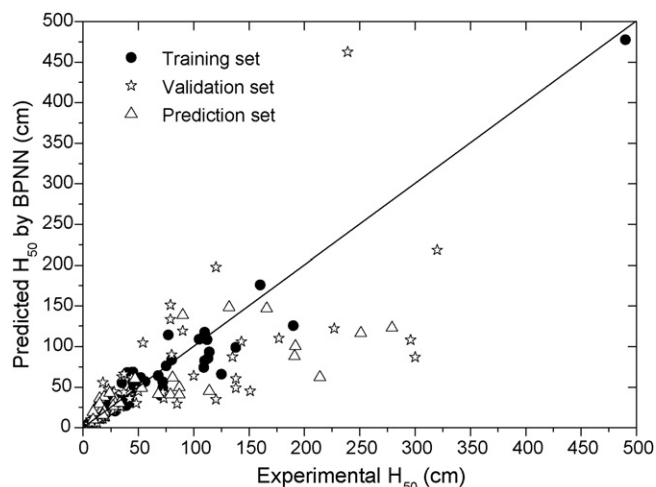


Fig. 4. Correlation between the predicted and experimental H_{50} by BPNN.

As for the work of Keshavarz and Jaafari [23], which built a QSPR model for prediction of impact sensitivity by employing 10 molecular descriptors and BPNN method, a general comparison is also presented. Firstly, we converted the impact sensitivity values of compounds from $\lg H_{50}$ to H_{50} (in cm). Following, the common compounds appeared in both works were collected as a new dataset and RMS errors of each model were calculated on them for comparison purpose. The new dataset includes 116 compounds in training set and 27 compounds in prediction set according to our dataset division. The new RMS errors for our model is 40 and 60 for training set and prediction set, respectively, while those for Keshavarz and Jaafari's model is 31 and 30, respectively. The results showed that our results are very close to those for the whole dataset (with the corresponding value of 43 and 58), while for the work of Keshavarz and Jaafari, the RMS error of the new dataset was much lower than that of the whole dataset (with RMS of 41). This fact may indicate the internal instability of the model of Keshavarz and Jaafari, because for stable models, the performances of subsets are always considered to be close to each other or to that of the whole dataset. Moreover, as recommended in literature [35], the model developed in this study has been tested by using a sufficiently large number of compounds not used in the model development (20% of the complete dataset), thus the developed model can be considered to be with a better external predictive ability and generalization performance.

4. Conclusion

In this study, the ETSI were successfully employed to build a QSPR model for predicting the impact sensitivity of nitro energetic compounds via BPNN. The results showed that the ETSI can well characterize the structure of nitro energetic compounds and there is a stronger non-linear relationship existed between ETSI and impact

sensitivity. Moreover, the BPNN model exhibited higher correlation coefficients and lower RMS than the MLR and PLS ones, which showed a better ability of prediction and generalization. However, due to the limited dataset employed in this work, it must be stated that the model developed cannot be applied for all nitro energetic compounds, such as polynitroheterocycles. Nevertheless, it can be still believed that the developed BPNN model using ETSI can well correlate the impact sensitivity with the molecular structure of nitro energetic compounds, and estimate the impact sensitivity of new nitro compounds or the ones whose experimental values are unknown.

Acknowledgements

This research was supported by the National Natural Science Fund of China (No. 50774048) and the Program for New Century Excellent Talents in University (No. NCET-05-0505). Y. Pan acknowledges the support of Jiangsu Graduate Scientific Innovation Projects (No. CX07B.150z).

References

- [1] P.A. Perssen, R. Holmberg, J. Lee, Rock Blasting and Explosives Engineering, CRC PRESS, Boca Raton, FL, 1993.
- [2] J.S. Li, G. Zeng, H.M. Xiao, et al., Quantum chemical study on the impact sensitivity of polynitroaromatics, Chin. J. Explos. Propellants 2 (1997) 56–61.
- [3] M.J. Kamlet, H.G. Adolph, The relationship of impact sensitivity with structure of organic high explosives, Propellants Explos. Pyrotech. 4 (1979) 30–34.
- [4] P. Politzer, J.S. Murray, P. Lane, et al., A relationship between impact sensitivity and the electrostatic potentials at the midpoints of C–NO₂ bonds in nitroaromatics, Chem. Phys. Lett. 168 (1990) 135–139.
- [5] P. Politzer, L. Abrahmsen, P. Sjöberg, Effects of amino and nitro substituents upon the electrostatic potential of an aromatic ring, J. Am. Chem. Soc. 106 (1984) 855–860.
- [6] P. Politzer, P.R. Laurence, L. Abrahmsen, et al., The aromatic C–NO₂ bond as a site for nucleophilic attack, Chem. Phys. Lett. 111 (1984) 75–78.
- [7] P. Politzer, J.S. Murray, Relationships between dissociation energies and electrostatic potentials of C–NO₂ bonds: Applications to impact sensitivities, J. Mol. Struct. 376 (1996) 419–424.
- [8] P. Politzer, P. Lane, Comparison of density functional calculations of C–NO₂, N–NO₂ and C–NF₂ dissociation energies, J. Mol. Struct. 388 (1996) 51–55.
- [9] P. Politzer, J.S. Murray, in: P.L. Markinas (Ed.), Organic Energetic Compounds, Nova Science Publishers, New York, 1996.
- [10] B.M. Rice, J.J. Hare, A quantum mechanical investigation of the relation between impact sensitivity and the charge distribution in energetic molecules, J. Phys. Chem. A 106 (2002) 1770–1783.
- [11] H.M. Xiao, Z.Y. Wang, J.M. Yao, The theoretical study on sensitivity and stability of polynitro arenes. I. Nitro derivatives of amino-benzenes, Acta Chim. Sinica 43 (1985) 14–18.
- [12] J. Fan, H.M. Xiao, Theoretical study on pyrolysis and sensitivity of energetic compounds. 2. Nitro derivatives of benzene, J. Mol. Struct. (THEOCHEM) 365 (1996) 225–229.
- [13] H.M. Xiao, J.F. Fan, Z.M. Gu, et al., Theoretical study on pyrolysis and sensitivity of energetic compounds. 3. Nitro derivatives of amino-benzenes, Chem. Phys. 226 (1998) 15–24.
- [14] J. Fan, Z. Gu, H.M. Xiao, et al., Theoretical study on pyrolysis and sensitivity of energetic compounds. Part 4. Nitro derivatives of phenols, J. Phys. Org. Chem. 11 (1998) 177–184.
- [15] Z.X. Chen, H.M. Xiao, S.L. Yang, Theoretical investigation on the impact sensitivity of tetrazole derivatives and their metal salts, Chem. Phys. 250 (1999) 243–248.
- [16] X.C. Zhao, H.M. Xiao, Impact sensitivity and activation energy of pyrolysis for tetrazole compounds, Int. J. Quantum Chem. 79 (2000) 350–357.

- [17] C.Y. Zhang, Y. Shu, Y. Huang, et al., Theoretical investigation of the relationship between impact sensitivity and the charges of the nitro group in nitro compounds, *J. Energ. Mater.* 23 (2005) 107–119.
- [18] C.Y. Zhang, Y. Shu, Y. Huang, et al., Investigation of correlation between impact sensitivities and nitro group charges in nitro compounds, *J. Phys. Chem. B* 109 (2005) 8978–8982.
- [19] C.Y. Zhang, Y. Shu, X. Wang, et al., A new method to evaluate the stability of the covalent compound: by the charges on the common atom or group, *J. Phys. Chem. A* 109 (2005) 6592–6596.
- [20] M.H. Keshavarz, Prediction of impact sensitivity of nitroaliphatic, nitroaliphatic containing other functional groups and nitrate explosives, *J. Hazard. Mater.* 148 (2007) 648–652.
- [21] H. Nefati, J.M. Cense, J.J. Legendre, Prediction of the impact sensitivity by neural networks, *J. Chem. Inf. Sci.* 36 (1996) 804–810.
- [22] S.G. Cho, K.T. No, E.M. Goh, et al., Optimization of neural networks architecture for impact sensitivity of energetic molecular, *Bull. Korean Chem. Soc.* 26 (2005) 399–408.
- [23] M.H. Keshavarz, M. Jaafari, Investigation of the various structure parameters for predicting impact sensitivity of energetic molecules via artificial neural network, *Propellants Explos. Pyrotech.* 31 (2006) 216–225.
- [24] L.H. Hall, L.B. Kier, Electrotopological state indices for atom types: a novel combination of electronic, topological, and valence state information, *J. Chem. Inf. Comput. Sci.* 35 (1995) 1039–1045.
- [25] L.H. Hall, C.T. Story, Boiling point and critical temperature of a heterogeneous data set: QSAR with atom type electrotopological state indices using artificial neural networks, *J. Chem. Inf. Comput. Sci.* 36 (1996) 1004–1014.
- [26] J. Huuskonen, M. Salo, J. Taskinen, Aqueous solubility prediction of drugs based on molecular topology and neural network modeling, *J. Chem. Inf. Comput. Sci.* 38 (1998) 450–456.
- [27] J. Huuskonen, Estimation of aqueous solubility for a diverse set of organic compounds based on molecular topology, *J. Chem. Inf. Comput. Sci.* 40 (2000) 773–777.
- [28] J. Huuskonen, D.J. Livingstone, I.V. Tetko, Neural network modeling for estimation of partition coefficient based on atom-type electrotopological state indices, *J. Chem. Inf. Comput. Sci.* 40 (2000) 947–955.
- [29] J. Huuskonen, QSAR modeling with the electrotopological state: TIBO derivatives, *J. Chem. Inf. Comput. Sci.* 41 (2001) 425–429.
- [30] J. Huuskonen, QSAR modeling with the electrotopological state indices: predicting the toxicity of organic chemicals, *Chemosphere* 50 (2003) 949–953.
- [31] Y. Pan, J.C. Jiang, R. Wang, et al., Prediction of auto-ignition temperatures of hydrocarbons by neural network based on atom-type electrotopological-state indices, *J. Hazard. Mater.* 157 (2008) 510–517.
- [32] C.B. Storm, J.R. Stine, J.F. Kramer, Sensitivity relationships in energetic materials, in: S.N. Bulusu (Ed.), *Chemistry and Physics of Energetic Materials*, Kluwer Academic Publishers, Dordrent, 1990, pp. 623–627.
- [33] Y. Pan, J.C. Jiang, Z.R. Wang, Quantitative structure–property relationship studies for predicting flash points of alkanes using group bond contribution method with back-propagation neural network, *J. Hazard. Mater.* 147 (2007) 424–430.
- [34] A. Tropsha, P. Gramatica, V.K. Gombar, The importance of being earnest: validation is absolute essential for successful application and interpretation of QSPR models, *QSAR Comb. Sci.* 22 (2003) 69–77.
- [35] P. Gramatica, Principles of QSAR models validation: internal and external, *QSAR Comb. Sci.* 26 (2007) 694–701.
- [36] S. Wold, L. Eriksson, Statistical validation of QSAR results, in: H. van de Waterbeemd (Ed.), *Chemometrics Methods in Molecular Design*, VCH, Weinheim (Germany), 1995, pp. 309–318.